Synthesis and photophysical properties of conjugated anthracene-based compounds

Assunta Marrocchi [a,b], Anna Spalletti [a,b,*], Serena Ciorba [a,b], Mirko Seri [a], Fausto Elisei [a,b], Aldo Taticchi [a,b]

[a] Dipartimento di Chimica, Università degli Studi di Perugia, Via Elce di Sotto, 8, 06123 Perugia, Italy
[b] Centro di Eccellenza Materiali Innovativi Nanostrutturati (CEMIN), Università degli Studi di Perugia, 06123 Perugia, Italy

ARTICLE INFO

ABSTRACT

Four novel diarylanthracene derivatives (**1**, **5a**, **5b**, **6**) have been synthesized by Suzuki and Sonogashira coupling reactions, characterized and their structure assigned by ^{1}H and ^{13}C NMR spectroscopy. The spectral and photophysical properties of a series of symmetrically and asymmetrically disubstituted anthracene-based compounds (**1–6**) and of benzothiadiazole derivative **7** have been studied. All these photostable systems show high fluorescence emission and a batochromic shift of the absorption spectrum that increase with π-conjugation. Flash photolysis measurements were carried out on the poor fluorescent compound **4**.

© 2010 Elsevier B.V. All rights reserved.

1. Introduction

Organic materials characterized by an extended π-conjugation are extensively investigated for their applications in organic and molecular electronics [1]. Considerable efforts have been directed towards the synthesis as well as the study of the photophysical properties of different types of molecular and polymeric conjugated systems, with the aim to exploit their potential as materials for efficient, stable, and easy processable devices.

Soluble organic molecules are promising materials for electronics since they can be deposited from solution, e.g. by a printing process, and are therefore compatible with low cost roll-to-roll fabrication technology [2]. Moreover, they offer advantages over polymeric materials in terms of easy synthesis and purification, and generally exhibit high charge carrier mobilities. Most important, molecular materials do not suffer from the structural variability of polymers, namely the control of regioregularity, molecular weight and polydispersity.

Recently [3] we described the synthesis of a series of anthracene-containing semiconductors, and their use as active layer in OTFTs as well as photovoltaic devices. Anthracene derivatives may exhibit large charge carrier mobility and excellent stability. Moreover, they generally show very high photo-luminescence quantum yield. Indeed, we demonstrated that soluble one-dimensional π-conjugated anthracene derivatives with acetylenic triple bonds as conjugation bridges, are promising candidates for organic semiconductors.

The present report deals with the synthesis and photophysical properties of the new anthracenes **1**, **5a**, **5b** and **6** (Fig. 1), to further elucidate architecture-electronic properties relationships within this semiconductor class. The detailed study of the spectral and photophysical properties of these compounds has been also extended to the anthracenes **2–4** [3d–f] (Fig. 1), with the aim to evidence the relationship between molecular structure and properties of the excited states in order to drive next syntheses towards compounds more useful as active materials in optoelectronics.

In particular, the design of the rod-shaped derivatives **1–4**, involves the extension of the π-conjugation of anthracene unit by introducing aryl groups at the 9- and 10-positions, that are connected by saturated or multiple linkages. The addition of end hexyloxy-chains to the backbone is expected to favour the ordered arrangements of the molecules in their solid state [4], which facilitates the charge transport through their π–π orbital stacking. These groups might also increase the material solubility, so that solution-processable devices may be fabricated.

Asymmetrically substituted systems **5a** and **5b** were also synthesized, as analogues of compound **2** in which an electron acceptor group replaces the alkoxy chains at one end of the molecule; though investigated for decades, interest in push-pull chromophores, with strong electron-donors and electron-acceptors connected by π-conjugating spacers, is still growing, in view of their outstanding
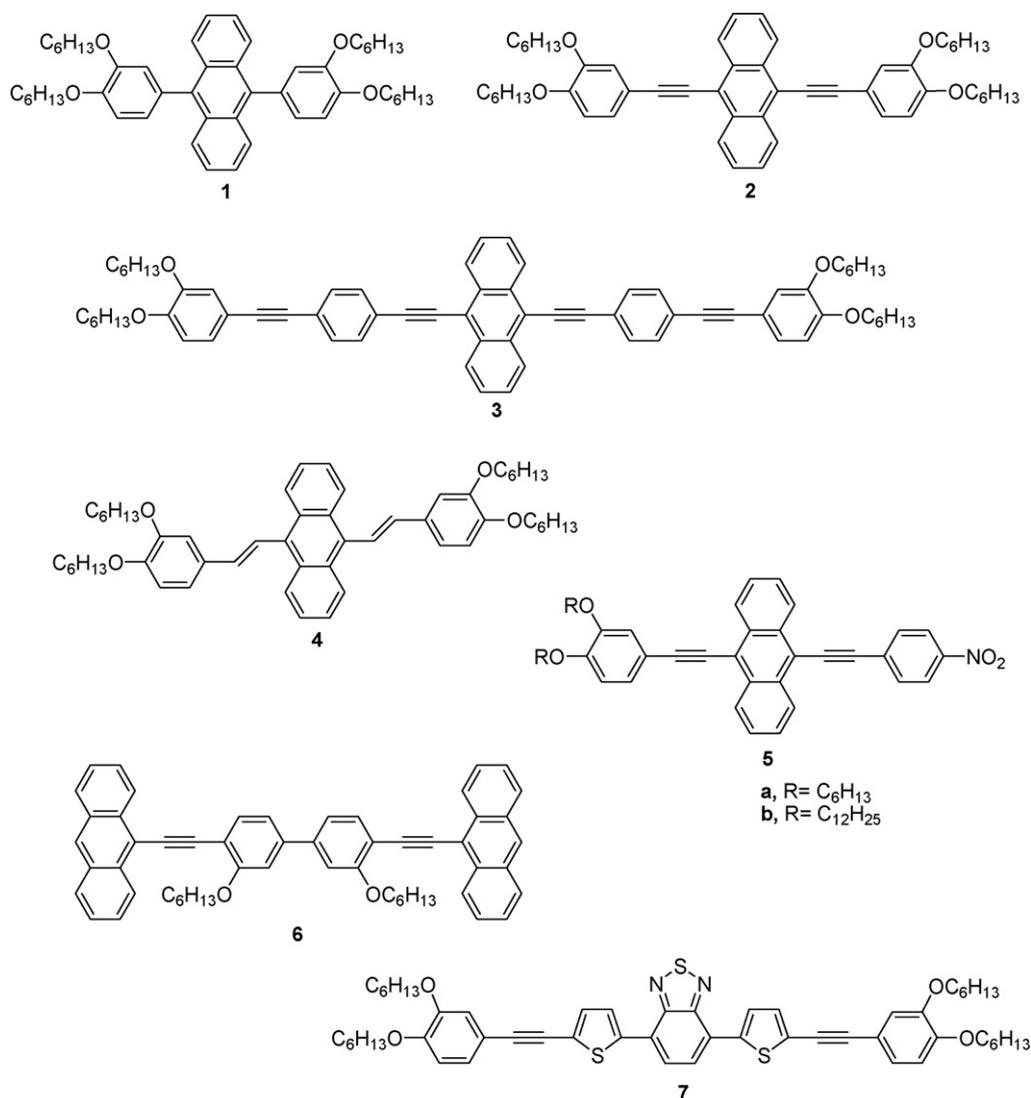
Fig. 1. Investigated compounds.

opto-electronic properties, in particular their non-linear optical behaviour, and their potential for application as advanced functional materials in molecular devices [1].

The doubly end-capped dianthryl compound **6** has been also considered, in order to study the effect of the terminal anthracene moieties on the spectral properties.

Finally, the comparison of the spectral and photophysical properties of compounds **2** and **3** with those of **7**, in which the anthryl core has been replaced by a benzothiadiazole unit [3f], allows to get information on the effects of fluorophore substitution.

2. Materials and methods (experimental)

2.1. General

Melting points (uncorrected) were determined by a Büchi melting point apparatus. Chromatography was performed by Riedel de Haën silica gel (230–400 mesh ASTM). Commercially available reagents (Sigma–Aldrich Co.) were utilized without further purification, unless otherwise noted. Petroleum ether as the 40–60 °C boiling fraction was used. NMR spectra were recorded by a Varian Associates VXR-400 multinuclear instrument (internal Me$_4$Si).

A PerkinElmer Lambda 800 spectrophotometer was used for the absorption measurements. The fluorescence spectra were recorded by a Spex Fluorolog-2 F112AI spectrofluorimeter. Dilute solutions (absorbance less than 0.1 at λ_{exc}) were used for fluorimetric measurements. 9,10-Diphenylanthracene and tetracene in air-equilibrated cyclohexane were used as fluorimetric standards ($\phi_F = 0.73$ [5] and 0.17 [6], respectively). Fluorescence lifetimes were measured by an Edinburgh Instrument 199S spectrofluorimeter, equipped with a pulsed lamp, filled by N$_2$ or H$_2$, using the single photon counting method (time resolution $\cong 0.5$ ns). All the photophysical measurements were carried out at room temperature in spectroscopic grade cyclohexane and chloroform, from Fluka. When required, the solutions were de-aerated by purging with pure nitrogen. The fluorescence quantum yields and lifetimes are averages of at least three independent experiments with mean deviation of ca. 10%.

For time-resolved laser flash photolysis measurements on the nanosecond time scale, the third harmonic ($\lambda_{exc} = 355$ nm) from a Continuum Surelite Nd:YAG laser was used with the energy less than 1mJ per pulse and 10 ns time resolution. Spectrophotometric analysis was performed by using a 150 W Xenon source, a Baird-Tatlock monochomator, a Hamamatsu R29 photomultiplier and a Tektronix DSA 602 digital analyzer.

Scheme 1.

The $\Phi_T \times \varepsilon_T$ product, for compound **4**, was determined by using anthracene in cyclohexane as a standard ($\varepsilon_{TT} = 4.55 \times 10^4 \, M^{-1} \, cm^{-1}$ at 432.5 nm, $\Phi_T = 0.71$) [7]. The molar absorption coefficient of the triplet state (ε_{TT}) was determined through a sensitization method by using anthracene as a sensitizer.

The quantum-mechanical calculations were performed by using the Hyper-Chem computational package (version 6.1): the heats of formation and dipole moments were obtained for geometries optimized by the PM3 method. The electronic spectra (transition energies and oscillator strengths) were calculated by ZINDO/S at the optimized geometries. Calculations of the configuration interaction included 1600 (40 × 40) single excited configurations. For **7** the starting conformations of minimal energy to be used for the optimization procedure were obtained by Conformational Search analysis (MM+ method).

2.2. Synthesis

9,10-Di[3,4-dihexyloxyphenyl]anthracene (1). To a solution of boroderivate **8** (0.404 g, 1 mmol) in dry toluene (3 ml) and under Ar atmosphere, was added 9,10-dibromoanthracene (**9**) (0.134 g, 0.4 mmol), Aliquat (0.081 g, 0.2 mmol) and Pd(PPh$_3$)$_4$ (0.046 g, 0.04 mmol). To this mixture was added a 1 M Na$_2$CO$_3$ aqueous solution (17 ml) degassed for 2 h. The mixture was then stirred for 24 h under reflux. The aqueous layer was extracted with CH$_2$Cl$_2$. The organic layer was dried with Na$_2$SO$_4$, filtered and concentrated in vacuo. The crude product was purified by column chromatography on silica gel, eluting with petroleum ether/CH$_2$Cl$_2$ 5:1 to afford 0.150 g of **1** (55% yield); recrystallization from EtOAc gave **1** as white crystals; m.p. 159–160 °C (ethyl acetate); ^{1}H NMR (CDCl$_3$) δ 0.82–0.84 (m, 6H), 0.89–0.93 (m, 6H), 1.25–1.57 (m, 24H), 1.75–1.82 (m, 4H), 1.85–1.93 (m, 4H), 3.87–4.00 (m, 4H), 4.09–4.13 (m, 4H), 6.92–6.96 (m, 4H), 7.05–7.07 (m, 2H), 7.27–7.31 (m, 4H), 7.72–7.76 (m, 4H); ^{13}C NMR (CDCl$_3$) δ 14.0, 22.6, 22.7, 25.7, 25.8, 29.2, 29.4, 31.6, 31.7, 69.2, 69.3, 113.5, 116.8, 123.6, 124.9, 127.1, 130.1, 131.5, 137.0, 148.5, 148.9; Anal. calcd. for C$_{50}$H$_{66}$O$_4$: C, 82.15; H, 9.10. Found: C, 82.00; H, 9.09%.

9-(3,4-Dihexyloxyphenylethynyl)-10-(p-nitrophenyl-ethynyl)anthracene (5a). Prepared by coupling compound **12** and 1,2-dihexyloxy-4-ethynylbenzene (**13a**) (1/1.1) following the above procedure. Reaction time: 18 h. Reaction temperature 50 °C; m.p.: 134–135 °C (ethyl acetate); ^{1}H NMR (CDCl$_3$) δ: 8.65 (m, 2H), 8.55 (m, 2H), 8.24 (d, J = 8.8 Hz, 2H), 7.80 (d, J = 8.7 Hz, 2H), 7.61 (m, 4H), 7.30 (d, 1H), 6.88 (d, 1H), 4.01 (m, 4H), 1.82 (m, 4H), 1.62–1.20 (m, 10H), 0.87 (s, 6H); ^{13}C NMR (CDCl$_3$) δ: 150.4, 148.9, 147.0, 132.4, 132.1, 130.3, 127.6, 127.3, 126.7, 125.4, 123.8, 120.6, 116,7, 116.2, 115.2, 113.3, 103.9, 100,0, 92.0, 84.8, 69.5, 69.2, 31.6, 29.2, 29.1, 25.7, 22.6, 14.0; UV–vis (CHCl$_3$) [λ_{max} nm (log ε)] 278 (4.8), 315 (4.3), 474 (4.6). An. Calcd. For C$_{42}$H$_{41}$NO$_4$: C, 80.87; H, 6.63; N, 2.25. Found: C, 80.99; H, 6.62; N, 2.23%.

9-(3,4-Didodecyloxyphenylethynyl)-10-(p-nitrophenyl-ethynyl)anthracene (5b). Prepared by coupling compound **12** and 1,2-didodecyloxy-4-ethynylbenzene (**13b**) (1/1.1) following the procedure described for reaction between **11** and **10**. Reaction time: 18 h. Reaction temperature 50 °C. Purified by crystallization from toluene; 86% yield (red crystals); m.p. 125–126 °C (toluene); ^{1}H NMR (CDCl$_3$) δ 8.70 (m, 2H), 8.57 (m, 2H), 8.27 (d, J = 8.9 Hz, 2H), 7.85 (d, J = 8.9 Hz, 2H), 7.63 (m, 4H), 7.30 (m, 1H), 7.20 (m, 1H), 6.89 (m, 1H), 4.03 (m, 4H), 1.81 (m, 4H), 1.45 (m, 4H), 1.22 (m, 32H), 0.82 (m, 6H); ^{13}C NMR (CDCl$_3$) δ 150.4, 148.9, 147.0, 132.4, 132.1, 131.8, 130.3, 127.5, 127.3, 126.7, 125.4, 123.8, 120.6, 116.8, 116.2, 115.2, 113.3, 103.9, 100.0, 92.0, 84.8, 69.5, 69.2, 47.9, 31.9, 29.7, 29.6, 29.4, 29.3$_4$, 29.3, 29.2, 26.0$_3$, 26.0, 22.6, 14.1; UV–vis (CHCl$_3$) [λ_{max} nm (log ε)] 278 (4.8), 472 (4.64). An. Calcd. for C$_{54}$H$_{65}$NO$_4$: C, 81.88; H, 8.27; N, 1.77. Found: C, 82.09; H, 8.26; N, 1.79%.

3,3'-Dihexyloxy-4,4'-diethynylanthracene-1,1'-biphenyl (6). Dry toluene (3 ml), 9-ethynyl-anthracene (**16**) (0.11 g, 0.52 mmol), CuI (0.002 g, 0.010 mmol), (0.15 g, 0.25 mmol), Pd(Ph$_3$)$_4$ (0.012 g, 0.010 mmol) and i-Pr$_2$NH (1.5 ml) were placed in a flask and degassed with Ar. The mixture was heated at 55 °C for 18 h,

5a: R=C$_6$H$_{13}$, 61%
b: R=C$_{12}$H$_{25}$, 75%

13 a: R=C$_6$H$_{13}$
b: R=C$_{12}$H$_{25}$
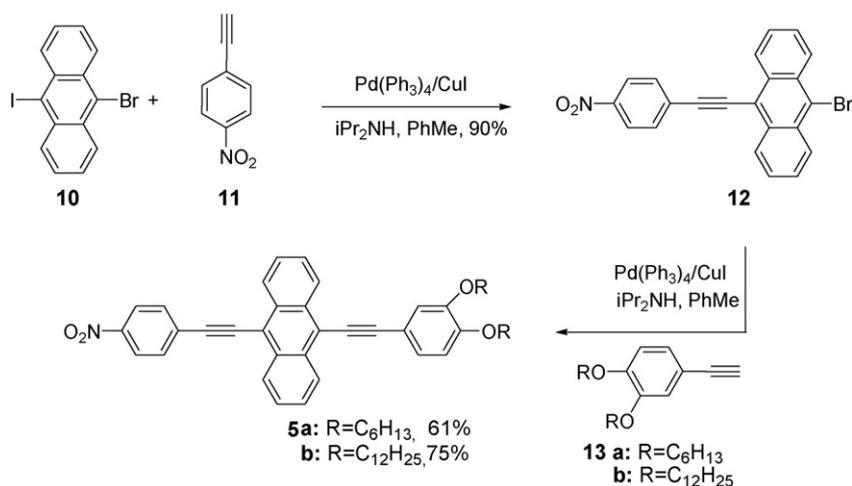
Scheme 2.

Scheme 3.
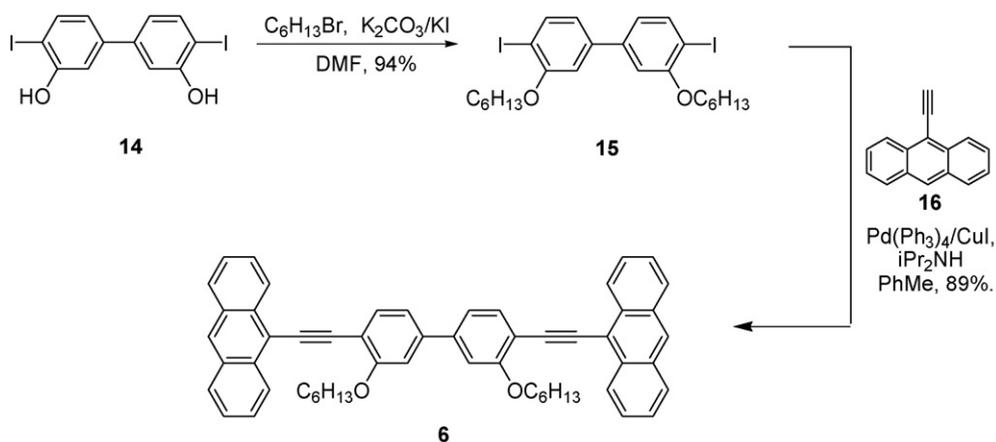
then the solvent was removed under reduced pressure and the residue was purified by column chromatography on silica gel (hexane/dichloromethane 85:15) to afford pure **6** as a yellow solid (62% yield); m.p. 203–204 °C (toluene); ^{1}H NMR (CDCl$_3$) δ 0.80 (m, 6H); 1.25–1.40 (m, 12H); 1.60 (m, 4H); 2.06 (m, 4H); 4.23 (m, 4H); 7.18 (m, 2H), 7.25 (m, 2H), 7.46–7.60 (m, 8H), 7.77 (m, 2H), 7.98 (d, 2H, J = 8.0 Hz), 8.38 (s, 2H), 8.78 (d, 2H, J = 8.8 Hz); ^{13}C NMR (CDCl$_3$) δ 165.3, 135.8, 131.5, 129.4, 128.6, 127.9, 126.7, 119.5, 96.7, 92.3, 68.9, 31.9, 28.8, 26.0, 23.2, 13.7. Anal. calcd. for C$_{56}$H$_{50}$O$_2$: C, 89.09; H, 6.68. Found: C, 88.95; H, 6.66%.

For details on the preparation of intermediate compounds **12** and **15** see Supporting Information.

3. Results and discussion

3.1. Synthesis

9,10-Diarylanthracene **1** was prepared by Suzuki cross-coupling reaction [8] between boro-derivative **8** and the commercial 9,10-dibromoanthracene (**9**) in the presence of the liquid phase-transfer catalyst Aliquat 336 (tricaprylmethylammonium chloride, A336) in two-phase solvent system (toluene/water) (Scheme 1). The boro-derivative **8** was synthesized starting from catechol according to previously described procedures [9].

The unsymmetrically substituted anthracene derivatives **5** were obtained by the repetitive Cu/Pd catalysed cross-coupling Sonogashira reaction [10]. Coupling reaction of 9-bromo-10-iodo-anthracene (**10**), prepared from 9,10-dibromoanthracene (**9**) [11], with *p*-nitro-ethynylbenzene (**11**) led to bromoarylethynyl anthracene **12** in high yield (90%) (Scheme 2). This compound was then subjected to coupling with 3,4-dialkoxyethynylbenzenes **13a** and **13b** to afford the diarylethynylanthracenes **5a** and **5b**, respectively, in high yield (61 and 75%) (Scheme 2).

3,3′-Dihexyloxy-4,4′-diarylethynylanthracene-1,1′-biphenyl (**6**) was synthesized by cross-coupling Sonogashira reaction between 3,3′-dihexyloxy-4,4′-diiodo-1,1′-biphenyl (**15**), obtained by the corresponding 4,4′-diiodo-3,3′-biphenol (**14**) [12], and 9-ethynyl-anthracene [13] (**16**) in good yield (62%) (Scheme 3).

The structures of all new compounds, i.e. **1**, **5a**, **5b**, **6**, **12** and **15** were unambiguously confirmed by ^{1}H and ^{13}C NMR spectroscopy and elemental analysis. Compounds **2**, **3**, **4** and **7** have been re-prepared according to previously reported procedures [3d–f].

3.2. Spectral behaviour

Normalized absorption and emission spectra of the investigated compounds in cyclohexane are shown in Figs. 2 and 3 and spectral properties are collected in Tables 1 and 2.
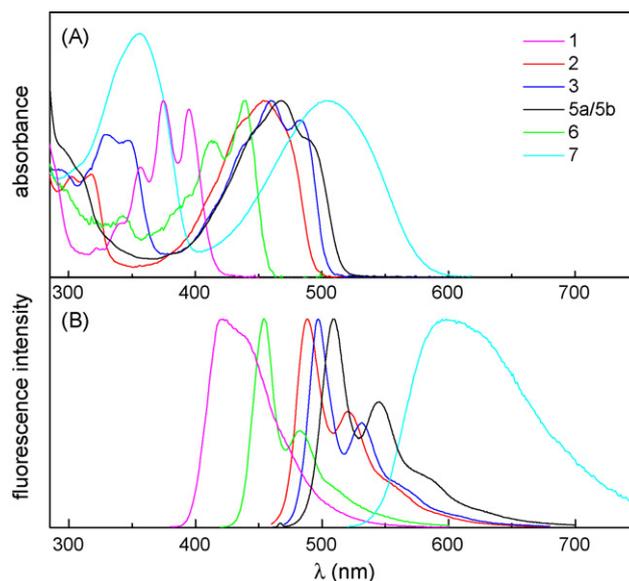
Fig. 2. Normalized absorption (A) and fluorescence emission (B) spectra of the studied compounds in cyclohexane at room temperature.
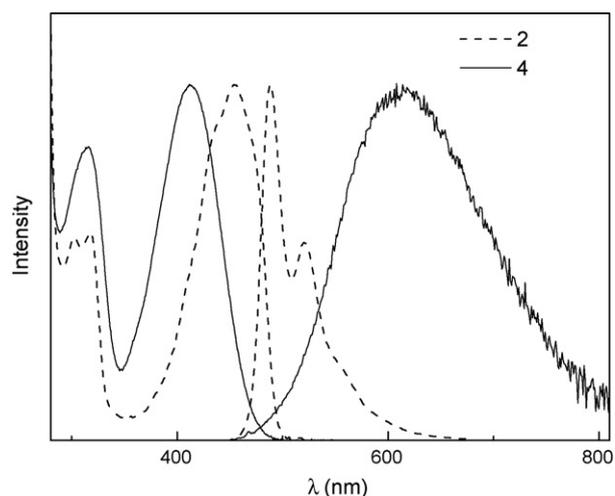
Fig. 3. Normalized absorption and fluorescence emission spectra of **4** in cyclohexane at room temperature (the spectra of **2** are reported for comparison).

Table 1
Absorption properties (absorption maxima wavelength, λ_{abs}^{max}, and coefficient, ε^{max}) of compounds **1**–**7** in chloroform at room temperature[a].

Compound	λ_{abs}^{max} (nm)	ε^{max} (10^4 M^{-1} cm^{-1})
1	292[sh], 34[sh], 359, <u>377</u>, 398	0.91, 0.45, 1.00, 1.65, 1.59
2	306, 322[sh], <u>457</u>, 475[sh]	2.44, 2.61, 4.30, 3.98
3	331, 349, 442[sh], <u>464</u>, 488	5.76, 5.47, 5.32, 7.19, 6.53
4	267, 317, <u>418</u>	9.50, 1.91, 2.36
5a	266[sh], 278, 315[sh], <u>472</u>, 494[sh]	5.57, 6.30, 2.30, 3.91, 3.52
5b	266[sh], 278, 315[sh], <u>473</u>, 494[sh]	5.59, 6.33, 2.32, 3.96, 3.57
6	300, 347, 393[sh], 419, <u>444</u>	1.55, 1.63, 2.36, 4.85, 6.58
7	<u>358</u>, 502	5.03, 3.72

[a] The underlined wavelengths refer to the main maxima, and *sh* means *shoulder*.

Except for **1** (which does not absorb at wavelengths larger than 420 nm), the absorption spectra generally show an intense band in the visible region, **2**, **3**, **5** and **7** having a second strong transition in the 290–400 nm range. Also the fluorescence spectra are intense, being the radiative process the largely main deactivation pathway, with the exception of the olefinic derivative **4** (see below). The spectra are shifted towards the red on increasing the extended conjugation through the system of aryl groups and triple bonds. The asymmetrically substituted compounds (**5**), containing a nitrogroup, show absorption and emission spectra red-shifted of about 15/20 nm with respect to the symmetric analogous **2**. The length of the side aliphatic chain ($-C_6H_{13}$ or $-C_{12}H_{25}$) does not affect the spectral behaviour of these compounds.

The spectra of anthracene derivatives are more or less structured (with the exception of **4**) with a vibronic progression of 1000–1400 cm^{-1} for the absorption ($\Delta\tilde{\nu}_{abs}$) and $\cong$1300 cm^{-1} for the emission ($\Delta\tilde{\nu}_F$), characteristic of a transition delocalized on the anthracene and the adjacent phenyl-triple-bonds moiety (see Scheme S1 in the Supporting Data) in the case of **2** and **3**, as found in the analogous unsubstituted 9,10-bis(phenylethynyl)anthracene [14a] (see Table 2).

The first transition of **1** is mainly localized in the anthryl group as evidenced by the typically structured absorption spectrum that shows vibronic peaks of feature and relative intensities similar to those of anthracene [14b], but red-shifted of about 20 nm, as confirmed by calculations (Scheme S2 in the Supporting Data).

In the case of **5a** and **5b**, the first absorption band is due to an allowed transition with a partial charge-transfer character as shown by calculations (Scheme S3).

The presence of two anthracene units in **6** does not cause a significant red shift of the absorption which however shows a very large absorption coefficient pointing to a spectral behaviour of **6** as due to two separate chromophores.

Compound **7** showed the most red-shifted absorption spectrum whose maximum well overlaps that of the solar spectrum.

The high absorption coefficients measured for these compounds (particularly in the case of **3**) and reported in Table 1 in chloroform, make them very useful as solar absorbers in photovoltaic devices.

The comparison between **2** and **4** spectra (Fig. 3) show that the replacement of two triple with two double bonds causes a
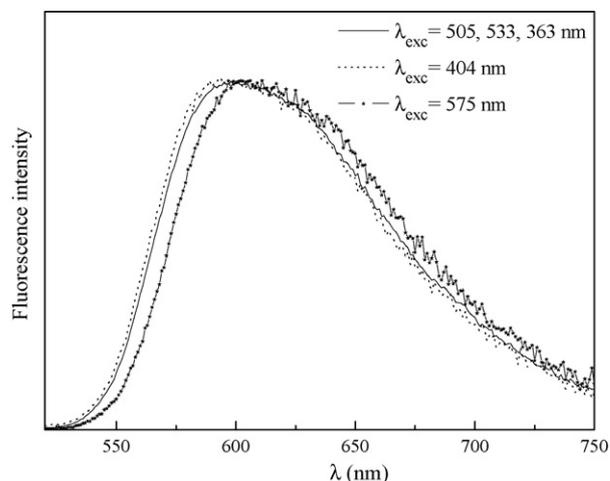

Fig. 4. Emission spectra of **7** in cyclohexane at room temperature as a function of λ_{exc}.

significant blue shift of the conjugation absorption band and the complete loss of the structure of the fluorescence spectrum that becomes a very large bell-shaped band with a strong displacement of the maximum towards the red. The blue shift of the absorption and the loss of resolution of both absorption and emission spectra could be explained by the presence of sets of non-planar structures caused by geometric distortions around the single bonds between the anthryl group and the ethenic carbons, as previously reported for the parent 9-styrylanthracene and analogous flexible compounds [15,16].

The huge Stokes shift observed for **4** (see Table 2) is reminiscent of a large one reported for the styrylanthracene in particular when the anthracene is length to the ethylenic bridge in 9 position [15,17]. An increase of planarity between the anthryl group and the two ethylenic bridges on excitation is probably responsible for this behaviour [15].

The experimental findings are nicely confirmed by calculations (see next section).

A negligible dependence of the shape of the fluorescence excitation and emission spectra on the emission wavelength (λ_{em}) and excitation wavelength (λ_{exc}), respectively, was found for all the investigated compounds, together with an excitation spectrum practically overlapping the absorption. This behaviour is probably due to the presence of a prevalent conformer or to very similar spectral properties of abundant species as discussed in Section 3.3. Only in the case of **7** the bell-shaped fluorescence spectrum is slightly affected by the excitation energy as shown in Fig. 4.

3.3. Quantum-mechanical calculations

The compounds **1**–**7** could exist, in principle, as mixtures of rotamers originated by the free rotation around quasi-single bonds

Table 2
Spectral behaviour of compounds **1**–**7** in cyclohexane at room temperature[a].

Compound	λ_{abs}^{max} (nm)	$\Delta\tilde{\nu}_{abs}$ (cm^{-1})	λ_F^{max} (nm)	$\Delta\tilde{\nu}_F$ (cm^{-1})	Stokes shift (cm^{-1})[b]
1	339, 357, <u>375</u>, 395	1350	<u>421</u>, 443[sh], 467[sh]	1200	2910 (1560)
2	433[sh], <u>454</u>, 478[sh]	1100	<u>488</u>, 521, 556[sh]	1300	1530 (430)
3	437[sh], <u>460</u>, 485	1100	<u>497</u>, 532, 561	1300	1620 (500)
4	413		615		7950
5a/5b	448[sh], <u>469</u>, 492[sh]	1000	<u>509</u>, 545, 586[sh]	1290	1680 (680)
6	391[sh], <u>413</u>, 439	1400	<u>454</u>, 482.5, 509[sh]	1300	750
7	505		600		3140

[a] The underlined wavelengths refer to the main maxima, and *sh* means *shoulder*.
[b] The values in parentheses refer to the Stokes shift calculated between the absorption and emission 0,0 transitions.
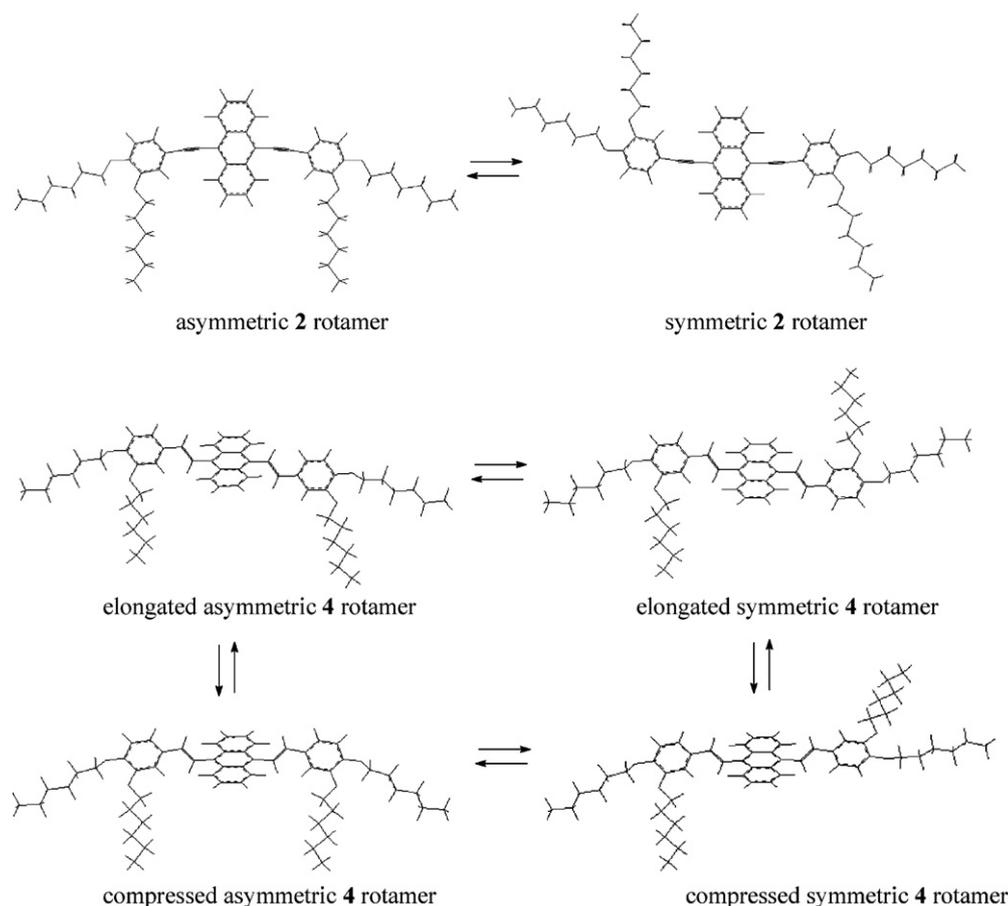
Fig. 5. Conformational equilibrium of **2** and **4**.

connecting aromatic groups and triple (or double) bonds [18,19]. The possible rotamers for the compounds **2** and **4** are reported in Fig. 5, as an example.

Table S1 reports the heat of formation, dipole moment and spectral properties calculated at the PM3 optimized geometries of the rotamers of the investigated compounds.

All the compounds were found to show a rigid and almost planar structure (neglecting the aliphatic chains) with the exception of compounds **1**, **4** and **7**.

The nitro-derivatives **5** exist as a unique conformer, the rotation around the quasi-single bond producing identical species. For **1** and the other symmetric compounds containing the anthracene group and triple bonds (**2**, **3**, **6**) the calculations showed that the two possible conformers with the aliphatic chains on the same (asymmetrical) or on the opposite (symmetrical) side with respect to the molecular long axis (e.g., see compound **2** in Fig. 5), have different dipole moments but identical absorption spectra, in agreement with the absence of wavelength effect on the excitation and emission spectra. More complex is the case of **4** (Fig. 5) and even more of **7**, where several conformers are expected to be present in the ground state. For **7** only the PM3 optimized and most stable conformation is reported in Fig. 6 and its relative calculated parameters in Table S1 (see Supplementary Data) [20]. The conformer with the planar central moiety with short intramolecular S···N contacts [20] (reported as the most stable in analogous compounds on the base of crystallographic data) [21] is placed at sizable higher energy by our calculations (PM3 method) indicating its negligible contribution to the conformational equilibrium in solution at room temperature. The calculations reproduce quite well the maxima of the experimental absorption spectra. Also the calculated oscillator strength (**f**) is reasonably in agreement with

the absorption coefficient reported in Table 1. As an example, the increase of the conjugation going from **2** to **3** causes an increase of **f** from 1.19 to 1.84, parallel to the increase of $\varepsilon^{\max}$ from 4.30 to $7.19 \times 10^4 \, M^{-1} \, cm^{-1}$.

Moreover, for the compound **1** having the lowest $\varepsilon^{\max}$ $(1.65 \times 10^4 \, M^{-1} \, cm^{-1})$ the smallest **f** $(\cong 0.4/0.5)$ was calculated.

3.4. Photophysical properties

The fluorescence parameters of the compounds **1–7** are reported in Table 3. These systems are efficient fluorophores, the high emission quantum yields being little affected by oxygen, as expected by the relatively short fluorescence lifetimes (in the range of few nanoseconds). The presence of the nitro-group does not affect the photobehaviour of these molecules, the fluorescence being the unique relaxation channel of their excited singlet state, contrary to the case of other nitro-derivatives where the emission decreases in favour of an efficient intersystem crossing (ISC) [22,23]. The emis-
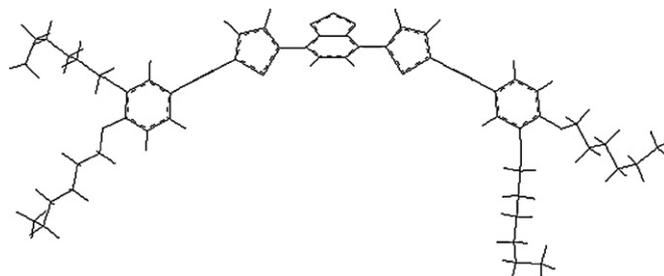

Fig. 6. Most stable conformation of **7**, as optimized by the PM3 method.

Table 3
Fluorescence parameters of compounds **1**–**7** in cyclohexane at room temperature.

Compound	ϕ_F	$\phi_F{}^a$	$\phi_F/\phi_F{}^a$	τ_F (ns)	k_F (10^8 s^{-1})
1	0.89	0.70	1.3	5.9	1.5
2	0.99	0.91	1.1	3.0	3.1
3	0.86	0.80	1.1	2.0	4.1
4	0.29	0.26	1.1	3.6	0.72
5a	1.00	0.93	1.1	3.0	3.3
5b	0.99	0.93	1.1	2.9	3.3
6	1.0	0.88	1.1	1.8	5.6
7	0.76	0.73	1.0	4.6	1.6

[a] In air-equilibrated solutions.

sion decay was mono-exponential for all compounds (χ^2 in the range 0.92–1.04, see Figs. S1–S7), in agreement with the negligible dependence of the fluorescence excitation and emission spectra on λ_{em} and λ_{exc}, respectively, and the calculation results that point to the presence of a prevalent species in the case of the olefinic derivative and to very similar spectral and photophysical properties of conformers of comparable abundance for the other acetylenic compounds. The measured lifetime for **7** is probably a mean value among quite similar lifetimes of several conformations.

All the compounds are photostable. No photoproducts were found under prolonged irradiation by monochromatic light at the absorption maximum. For compound **4**, this photostability (the disappearance yield, at $\lambda_{exc} = 436$ nm, is around 10^{-4} in cyclohexane) together with a reduced fluorescence quantum yield (see Table 3), points to the presence of non-reactive, non-radiative deactivation pathways of its excited states ($S_1 \rightarrow S_0$ internal conversion and/or $S_1 \rightarrow T_1$ intersystem crossing, ISC, to a non-reactive triplet state followed by ISC to the ground state), in analogy with the parent 9-styrylanthracene [24]. The transient spectrum of **4** observed on direct laser excitation ($\lambda_{max} = 490$ nm, see Fig. S8), was assigned to $T_1 \rightarrow T_n$ absorption since it was quenched by oxygen at nearly diffusion rate and generated by photosensitization using anthracene as triplet donor. $\varepsilon_{TT} = 4.8 \times 10^4$ M^{-1} cm^{-1} in cyclohexane at $\lambda_{max} = 490$ nm was determined for **4**, very similar to that of anthracene. The measured relatively low triplet quantum yield ($\phi_T = 0.01$) of **4** does not account for all the non-radiative decay pointing to a prevalent deactivation of the singlet excited state through internal conversion.

The high value of the fluorescence kinetic constant ($k_F = \phi_F/\tau_F$, $\cong 10^8$ s^{-1}) for all compounds **1**–**7** points to an allowed character of their emitting state, the same reached by absorption.

This is in agreement with the high oscillator strength calculated for the first transition (see Table 3). As a matter of fact, in the case of nitro-derivatives (**5a**/**5b**) the theoretical calculations predicted the presence of a lowest forbidden state around 500 nm. This behaviour can be understood taking into account the solvent effect on the state order which is inverted on going from gas-phase to solution [25].

4. Conclusions

In summary we have synthesized and characterized four new diarylanthracene derivatives. Photophysical properties and spectral behaviour of compounds **1**–**7** have been studied. The high fluorescence quantum yield of these photostable compounds make them interesting as good fluorescent probes.

The presence of side chains, necessary for solubility reasons and then for constructing electronic devices, does not affect the spectral and photophysical properties of these compounds that show absorption spectra in the visible region and very high fluorescence quantum yield. In the case of nitro-derivative the alkoxy chains work also as electron-donors in these push-pull systems, the partial charge-transfer character of the main UV–vis transition causing a further red-shift of the absorption spectrum.

Strong steric interactions occur when anthracene is placed between two single bonds, as in **1**, or two double bonds, as in **4**; this leads to a blue shift of the absorption spectra of approximately 70 nm, as compared with the case where anthracene is adjacent to two triple bonds (**2**). Indeed, the high absorption coefficient observed for anthracene-containing arylacetylenes **2** and **3** make them potentially useful solar absorbers in organic photovoltaic devices.

The replacement of the anthracene with a dithienylbenzothiadiazole unit in **2** causes a further significant red-shift of the absorption spectrum (more than 40 nm), pointing to the fact that compound **7** remains the most interesting for solar cells applications.

Appendix A. Supplementary data

Supplementary data associated with this article can be found, in the online version, at doi:10.1016/j.jphotochem.2010.03.002.

References

[1] Inter alia:
    (a) R.F. Service, Science 294 (2001) 2442;
    (b) H. Klank, Organic Electronics: Materials, Manufacturing, and Applications, Wiley-VCH, 2006;
    (c) G. Malliaras, R.H. Friend, Phys. Today 58 (2005) 53;
    (d) A. Facchetti, M.-H. Yonn, T.J. Marks, Adv. Mater. 17 (2005) 1705;
    (e) S. Günes, H. Neugebauer, N.S. Sariciftci, Chem. Rev. 107 (2007) 1324;
    (f) L. Zhao, J.-h. Zou, J. Huang, C. Li, Y. Zhang, C. Sun, X.-h. Zhu, J. Peng, Y. Cao, J. Roncali, Org. Electron. 9 (2008) 649;
    (g) J.A. Letizia, M.R. Salata, C.M. Tribout, A. Facchetti, M.A. Ratner, T.J. Marks, J. Am. Chem. Soc. 130 (2008) 9679;
    (h) J.L. Brusso, O.D. Hirst, A. Dadvand, S. Ganesan, F. Cicoira, C.M. Robertson, R.T. Oakley, F. Rosei, D.F. Perepichka, Chem. Mater. (2008) 2484;
    (i) M.L. Tang, A.D. Reichardt, N. Miyaki, R.M. Stoltenberg, Z. Bao, J. Am. Chem. Soc 130 (2008) 6064.
[2] D.R. Gamota, X. Kalyanasundaram, J. Zhang (Eds.), Printed Organic and Molecular Electronics, Kluver Academic, 2004.
[3] Inter alia:
    (a) L. Valentini, F. Mengoni, A. Taticchi, A. Marrocchi, S. Landi, L. Minuti, J.M. Kenny, New J. Chem. 30 (2006) 939;
    (b) L. Valentini, F. Mengoni, J.M. Kenny, A. Marrocchi, A. Taticchi, Small 3 (2007) 1200;
    (c) L. Valentini, F. Mengoni, F. Meloni, A. Marrocchi, M. Seri, A. Taticchi, J.M. Kenny, Thin Solid Films 516 (2008) 7193;
    (d) L. Valentini, D. Bagnis, A. Marrocchi, M. Seri, A. Taticchi, J.M. Kenny, Chem. Mater. 20 (2008) 32;
    (e) A. Marrocchi, A. Silvestri, M. Seri, A. Facchetti, A. Taticchi, T.J. Marks, Chem. Commun. (2009) 1380;
    (f) A. Marrocchi, M. Seri, C. Kim, A. Facchetti, A. Taticchi, T.J. Marks, Chem. Mater. 21 (2009) 2592.
[4] J. Locklin, M.E. Roberts, S.C.B. Mannsfeld, Z. Bao, Polym. Rev. 46 (2006) 79.
[5] G. Bartocci, F. Masetti, U. Mazzucato, A. Spalletti, I. Baraldi, F. Momicchioli, J. Phys. Chem. 91 (1987) 4733.
[6] J.B. Birks, Photophysics of Aromatic Molecules, Wiley-Interscience, London, 1970, p. 123.
[7] M. Montalti, A. Credi, L. Prodi, M.T. Gandolfi, Handbook of Photochemistry, Taylor & Francis, 2006, p. 231 and references therein.
[8] A.J. Suzuki, Organomet. Chem. 576 (1999) 147.
[9] (a) A. Loupy, J. Sansoulet, F. Vaziri-Zand, Bull. Soc. Chim. Fran. (1987) 1027;
    (b) M.D. McKenna, J. Barberà, M. Marcos, J.L. Serrano, J. Am. Chem. Soc. 127 (2005) 619.
[10] K. Sonogashira, in: F. Diederich, P. Stang (Eds.), Metal-Catalyzed Cross-Coupling Reactions, Wiley-VCH, Weinheim, 1988.
[11] E.E. Nesterov, Z. Zhu, T.M. Swager, J. Am. Chem. Soc. 127 (2005) 10083.
[12] A.C. Benniston, L. Peiyi, C. Sams, Tetrahedron Lett. 44 (2003) 3947.
[13] M.A. Heuft, S.K. Collins, G.P.A. Yap, A.G. Fallis, Org. Lett. 3 (2001) 2883.
[14] (a) I.B. Berlman, Handbook of Fluorescence Spectra of Aromatic Molecules, Academic Press, New York and London, 1971, pp. 369–370;
    (b) I.B. Berlman, Handbook of Fluorescence Spectra of Aromatic Molecules, Academic Press, New York and London, 1971, p. 356.

[15] G. Bartocci, F. Masetti, U. Mazzucato, A. Spalletti, G. Orlandi, G. Poggi, J. Chem. Soc. Faraday Trans. 2 84 (1988) 358, and references therein.
[16] G. Marconi, G. Bartocci, U. Mazzucato, A. Spalletti, F. Abbate, L. Angeloni, E. Castellucci, Chem. Phys. 196 (1995) 383, and references therein.
[17] H.-D. Becker, K. Sandros, L. Hansen, J. Org. Chem. 46 (1981) 821.
[18] U. Mazzucato, F. Momicchioli, Chem. Rev. 91 (1991) 1679.
[19] G. Bartocci, A. Spalletti, U. Mazzucato, in: J. Waluk (Ed.), Conformational Analysis of Molecules in Excited States, Wiley-VCH, New York, 2000 (chapter 5).
[20] A.S. Özen, C. Atilgan, G. Sonmez, J. Phys. Chem. C 111 (2007) 16362.

[21] M. Karikomi, C. Kitamura, S. Tanaka, Y. Yamashita, J. Am. Chem. Soc. 117 (1995) 6791, and references therein.
[22] H. Görner, F. Elisei, U. Mazzucato, G. Galiazzo, J. Photochem. Photobiol. A: Chem. 43 (1988) 139.
[23] I. Škorić, S. Ciorba, A. Spalletti, M. Šindler-Kulyk, J. Photochem. Photobiol. A: Chem. 202 (2009) 136.
[24] G. Galiazzo, A. Spalletti, F. Elisei, G. Gennari, Gazz. Chim. Ital. 119 (1989) 277.
[25] I. Baraldi, E. Benassi, S. Ciorba, M. Šindler-Kulyk, I. Škorić, A. Spalletti, Chem. Phys. 361 (2009) 61.